Design and Simulation of Valve Less PZT Micropump for Drug Delivery System

Manoj Pandey[1,*] and P.C. Upadhyay[1, 2]

[1]Department of Electronics and Communication Engineering

B K Birla Institute of Engineering and Technology (BKBIET), Pilani-333031, Rajasthan

[2]Department of Electronics and Communication Engineering

Sant Longowal Institute of Engineering and Technology (SLIET), Sangrur-148001, Punjab

[*]*Corresponding author*: manoj2pandey@yahoo.com

Abstract

In this paper some discrete parts of an electrostatic and flat-walled self-aligned valveless, micropump for drug delivery system is designed and simulated. The core component of the system is a piezoelectric diaphragm that can convert the reciprocating movement of a diaphragm actuated by a piezoelectric actuator into a pumping effect. The deflection in the diaphragm was analyzed by applying the voltages and pressures over different size of membrane. Nozzle/diffuser elements were used to direct the flow from inlet to outlet. Simulation was also done for a nozzle and diffuser element. A wide-angle flow channel with sharp inlet and outlets were used in the micropump with dynamic passive valves. The simulations shows differences in the flow patterns for diffuser and nozzle elements that explain the opposite positive flow directions. Numerical simulation were done using CFD program ANSYS. Based on the theoretical analysis, the effect of piezoelectric materials properties, driving voltage, driving frequency, nozzle/diffuser dimension, and other factors on the performance of the fluid system are discussed. As a result, a viable design and independent analysis for diaphragm and nozzle/diffuser with a flow channel of a micropump system for drug delivery is achieved.

Keywords: PZT micropumps; Diffuser-Nozzle; Valve-less Micropumps, Piezoelectric Actuators.

1. Introduction

Microfluidics has been established as a new engineering discipline with a huge scientific and commercial potential. In the last decades, research on microfluidic devices and fluidic phenomena in micro scale has become a strategic topic of the international research community. Based on silicon micro-fabrication techniques a number of different micropump designs have been presented [1, 2, 13]. However, the various micropumping technologies, mechanical micropumps with vibrating diaphragms have generated the most interest. Although, many novel pumping strategies such as pumps based on

growing and collapsing bubbles [3], electro hydrodynamics [4], electroosmosis [5] and flexural plate waves [6] have also been investigated. Most of these pumps are not able to produce high flow rates (of the order of several hundred μl/min to a few ml/min) which are easily achievable with mechanical micropumps. The described piezoelectricaly actuated valveless Micropumps (PAVMs) are a major research topic with a wide range of potential applications including but not limited to drug delivery, chemical synthesis, chemical detection, localized cooling of electronic circuits, microbiology, biological detection, clinical analysis in medicine and inkjet printing.

In the micro-electro-mechanical systems (MEMS) area, the piezoelectricaly actuated diaphragm has been widely used as an actuator to pump fluid in the microfluidic application. By the diaphragm deformation caused by the PZT actuator, the induced volume change of pressure chamber makes the pumping effect possible [4]. Since PAVMs have simple structure and no internal moving parts, therefore there is less risk of closing the valves when it pumps fluid containing particles. In addition they can respond quickly and have obvious advantages over other kinds of micropumps.

2. Design and Working Principle

Figure 1 shows a pictorial representation of the working principle of a PAVM the micropump can be understand very clearly with the help of the, which shows the, driven by a piezoelectric patch bonded to a diaphragm, which forces fluid through a small chamber. In parallel flow as shown in figure 1(a), in supply mode the flow rate through the nozzle is less than that trough the diffuser because resistance in the nozzle is higher than the resistance in the diffuser means $\Phi_i > \Phi_o$ and opposite in case of pump mode. Therefore, when the diaphragm deflects upwards in the first half cycle (figure 1(a)), more fluid will come into the chamber through the diffuser than through the nozzle. In the other half cycle, for pump mode the diffuser in the first half cycle acts as a nozzle when the diaphragm deflects downwards (figure 1(b)) and less fluid goes through it. Hence there is net flow through in the complete cycle.

The diffuser and nozzle structures are strongly dependent on the angle of the truncated pyramid. However the general flow in the enlarging or contracting direction is preferred. The flow is accelerated by sudden contraction at inlet in nozzle. Then the pressure drop across the duct increases the kinetic energy and thus also the flow velocity. The head loss is less in small opening angle (3^0) as compare to large taper angle of (35^0) [1, 3]. Koch and Evans compared the different tapered angle and head loss factor due to sudden contraction and expansion with gradual expansion and contraction. He concludes the flow is mainly dependent on the sudden contraction and expansion rather than the gradual contraction of the nozzle.
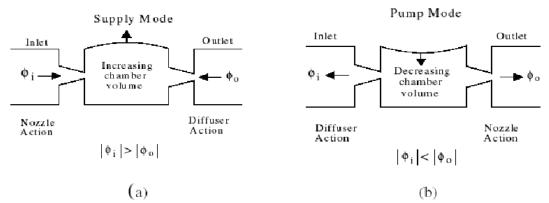
Fig:(1) Principle of operation for nozzle/diffuser valveless micropump; (a) supply mode (b) pump mode.

In order to keep the design simple, commercially available piezo discs were selected as actuators. A 100um thick piezo disc is consisted of a piezoelectric (PZT-5H) material glued over a silicon membrane of dimension of 7mm×4mm×70um by using conductive epoxy glue. The diffuser element is the important part of the valveless diffuser pump that gives the pump its flow directing properties. It consists of a diffuser, a flow channel with expanding cross-section in the positive direction, with a flat walled shape inlet and its reflected as outlet as shown in figure 2. The length of inlet at bottom is 620um and at top is 130um with a height of 550um with a distance of 2500um between inlet and outlet. The thickness of channel cross-section is taken as 30 um.
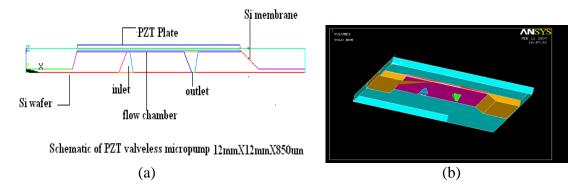

Fig 2. (a) Shows the schematic view of micropump in X-Z plane and (b) areas plot of complete micropump

3. Piezoelectric Actuator

3.1. *Cause of deflection*

The lead zirconate titanate (PZT) transducer has been widely used as an actuator to pump fluid in the microfluidic application. By the diaphragm deformation caused by the PZT actuator, the induced volume change of pressure chamber makes the pumping effect possible. Among those PZT deformation modes, the common type is the extension one because it is easily poled and commercially available. It has been usually designed with two shapes including the rod-shaped actuator and plate-shaped [7].

As an electric field is applied parallel to the polarization, they extend along its poling axis (d33 deformation) and also shrink in the lateral direction (d31 deformation) perpendicular to poling axis as shown in figure 3. These deformations are utilized to push or bend the diaphragm. Depending on how the actuator works to deform the diaphragm, this type of actuator is divided into three modes in this report, which are named by the "bend by d31 mode", the "push by d33 mode" and the "push by d31 mode". The d33 and d31 are the two normal piezoelectric coefficients to evaluate the extension or shrinkage. These modes of actuators must be directly attached to the diaphragm surface and so their sizes are confined to the diaphragm dimensions. The "bend by d31 mode" design has the plate-shaped actuator glued on the diaphragm to deform the diaphragm. With external electric field and polarization direction along its thickness direction, the extension difference between two layers leads to bending deformation. This mode is frequently used in microfluidic applications [1,3,7]. The other two "push mode" designs ("push by d31 mode" and "push by d33 mode") have actuators to deflect the diaphragm by means of the normal deformation along or perpendicular to the PZT polarization [1–3]. The membrane of the micro pump is actuated pizoelectrically. For mass production of the micropump, PZT can be printed onto the whole silicon wafer by the thick film technology. With a maximum drive voltage of 200 V, the maximum electrical field strength was 1.1kV/mm, which was lower than the break down field of most common piezoelectric material (>2 kv/mm). [5]. In this paper, we define the top electrode of the piezo disc as the voltage terminal and the silicon base material as ground terminal. The electric field applied on the PZT plate induced an expanding strain in the disc perpendicular to the electric field and a contracting strain in the direction of the disc thickness (assuming that the piezoelectric coefficient $d_{31}$is negative and d_{33} is positive). Since the piezoelectric layer was tightly glued on the silicon membrane there were reacting forces from the membrane opposing the expansion of PZT layer. This motional restriction causes the deflection of the disc.

3.2.   Results and Simulation

For the simulation point of view of the actuator a coupled field analysis for structure and electric is checked. A coupled field element solid 98 is used to model the membrane and PZT plate. The different material properties for Si membrane and PZT-5H are used for the analysis. Since bonding layer is very thick so it is neglected in FEM analysis. The fig 3(a) shows deflection with applying the pressure on the PZT plate (7mm×mm of the order of 1Kpa and boundaries are fixed in all degrees of freedom to observe the strain and stress distribution on the whole membrane. The maximum deflection is observed 23um at the centre of the actuator. The 2D bimorph beams (12mm×100um) have been simulated by applying the driving voltage of 200V. The piezoelectric element plane 223 has taken for the coupled field

piezoelectric analysis and the material properties are shown in table 1 and table 2. All the boundary conditions are applied with fixed the ends of bimorph. The vector and contour plot of beam are shown in figure 3(a) and 3(c) respectively. The maximum deformation obtained is 1.08 micron at the centre of beam. Fig 3 (b) shows the voltage distribution profile for the piezoelectric electrode, while top layer is applied as 200V and bottom is grounded. In the similar way the three dimensional (3D) simulations of designed diaphragm are shown in figure 4. The considered material properties of 3D simulation is summarised in table 2.

Table 1 Material Property for Two Dimensional Bimorph [10]

Piezo Mat (PIEZ) Table For Material 1 Piezoelectric strain matrix [d]				Piezoelectric stress matrix [e] computed from the piezoelectric strain matrix [d] and anisotropic elasticity matrix				D Matrix (ANEL) Table For Material 1	Dielectric Permittivity, at constant stress	
	X	Y	Z		X	Y	Z	D11 0.50000E-09	EP11	EP22
X	0.0000	0.22000E-10	0.0000	X	0.0000	0.28756E-01	0.0000	D12 -0.14500E-9	12.000	12.000
Y	0.0000	-0.30000E-10	0.0000	Y	0.0000	-0.51864E-01	0.0000	D13 -0.14500E-9		
Z	0.0000	0.30000E-11	0.0000	Z	0.0000	-0.70137E-03	0.0000	D22 0.50000E-9		
								D23 -0.14500E-9		
								D33 0.50000E-9		
								D44 0.12903E-08		

EVALUATE MATERIAL PROPERTIES FOR MATERIALS   1 TO   2 IN INCREMENTS OF 1
 MATERIAL NUMBER = 2 EVALUATED AT TEMPERATURE OF   0.0000
  EX   = 0.16800E+12
  NUXY = 0.30000
  PRXY = 0.30000

Table 2 Properties of Different Materials Used

Material	Property	Tensor(in order of x,y,z,xy,yz,xz)
PZT (5H) plate	Piezoelectricity e (cm^{-2})	0.0 0.0 -5.4 0.0 0.0 -5.4 0.0 0.0 15.8 0.0 0.0 0.0 0.0 12.3 0.0 12.3 0.0 0.0
	Permitivity ε (F^{m-1}) $\times 10^{-9}$	8.107 0 0 0 8.107 0 0 0 7.346

	Compliance S ($m^2 N^{-1}$) $\times 10^{-12}$	16.4 -5.75 -8.45 0 0 0
		 0 16.4 -8.45 0 0 0
		          18.8 0 0 0
		Symmetry 44.3 0 0
		                  47.5 0

		47.5
	Density (Kgm^{-3})	7500
	Poison's ratio	0.3
	Young's modulus E (GPa)	126
Silicon membrane	Density (Kgm^{-3})	2300
	Young's modulus E (GPa)	168
	Poisson's ratio	0.2

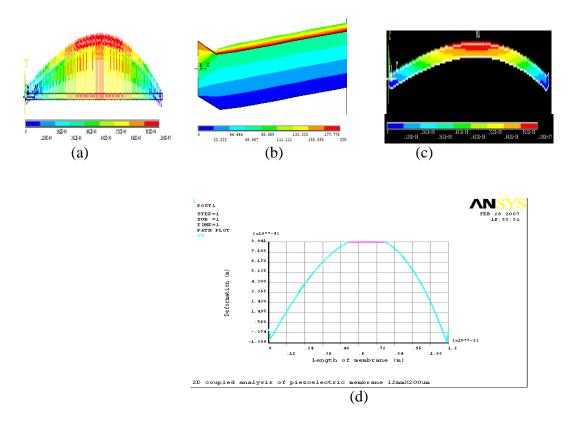(a)   (b)   (c)

(d)

Fig.3: 2D simulated results of 12mm×100um bimorph with applied peak to peak voltage 200 V when ends are fixed.(a):deflected beam vector plot ;(b)contour plot of voltage distribution Si base to PZT layer ;(c) contour plot for bending moment of bimorph; (d) Graph plot between length of bimorph(mm) and deflection (microns).

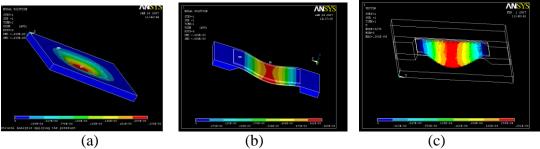(a)   (b)   (c)

Fig: 4 (a) deformation of a rectangular PZT plate (7mmx4mmX100um) glued over the Si material (12mmX8mmX70um) with applied load of 1KP pressure when boundaries are fixed, (b) deformation of a PZT actuator (7mmx4mmX100um) glued over the Si membrane (12mmX8mmX70um) with applied load of 200V peak-to-peak voltage when boundaries are fixed and (c) Vector plot of membrane deformation of the micropump for the figure 3 (b).

4. Nozzle/Diffuser

By definition, a diffuser is a device for reducing the velocity and increasing the static pressure of a fluid passing through a system i.e it transforms kinetic energy to potential energy. Diffusers and nozzles are common devices in internal volume flow systems. The flow rate of a valveless micropump depends on the rectification efficiency of the pump among other factors (such as amplitude and frequency of operation of the diaphragm). The rectification effienciency is calculated and analyzed by Anders Olsson [3]. Many microfluidic devices cannot be described by either a simple laminar or turbulent model, because the length of the element in the flow direction is shorter than the entrance length for fully developed laminar or turbulent flow. The simulations were done using a Dell PentiumPro 200 MHz. The version of ANSYS Multiphysics 8.0 used allowed models with a maximum of approximately 20,000 elements in FORTRAN. Simulations were done using both two- and three-dimensional models. The drawback with three-dimensional models is that 20,000 elements give only 27 elements per dimension if they are equally spaced. A two-dimensional model increases the possible grid size to 141. For the three-dimensional model, the mesh was chosen to have the number of elements close to 20,000 with the finest mesh at the highest velocity gradients. For the two-dimensional models, between 10,000 and 20,000 elements were used. The two-dimensional model also had greater freedom in the allowed element shapes. The laminar and turbulent simulations did not differ significantly and for the diffuser elements with other geometrical dimensions, simulations were only done using laminar flow. The simulations were done for the pressure range 0–100 KPa using two-dimensional models and for Reynolds numbers below 400 using three-dimensional models.

4.1 Results and Simulation

In this section of the paper some simulated results of the nozzle and diffuser part have shown to find the required pump. The 3-D simulation of nozzle of height 550 micron, pyramidal shape is simulated. The CFD/FLOTRAN simulation using 3D element fluid 142 flow analysis with air-in. Set all the material properties like viscosity and density for air-in for fluid flow and applied the boundary conditions. The initial velocity is applied at inlet of the order of microns/liter and 0 pa backpressure at outlet. The result shows that flow rate is maximum towards the outlet.
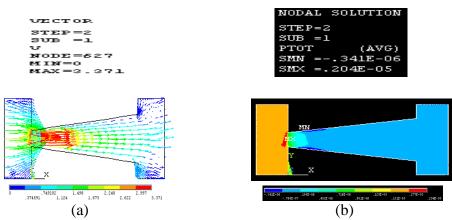
(a)   (b)

Fig. 5: Flow patterns simulated plot for two-dimensional model of length 20mm, opening angle 9.8^0 and smallest width is 130um. (a) Velocity vector plot with entering velocity 1ml/s and 0backpressure at opening end. (b) Contour plot for the pressure distribution for the same load.

(a)   (b)   (c)
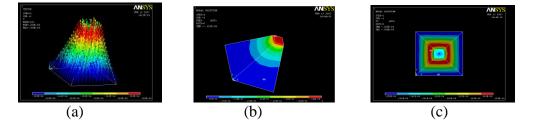
Fig. 6. (a) Flow rate vector plot of nozzle. (b) Pressure Contour plot of nozzle (c) velocity contour.

Typical simulated flow patterns for a diffuser element of in a diffuser pump are shown in Figure 5. The velocity is reduced before the exit in the positive diverging-wall direction before the remaining kinetic energy is lost in a jet at the outlet. In other hand the flow velocity in increasing towards the converging of the nozzle as shown in figure 6.   In the converging-wall direction, the flow is accelerated through the nozzle to high velocity and the kinetic energy is lost in a jet at the outlet. In the diverging-wall direction, the laminar solution shows a small asymmetry at the outlet that is not seen for the turbulent solution. The pressure distribution is shown for the same condition in Figure 5(b) for 2D and figure 6 (b) for 3D simulations. The diverging-wall direction is the positive flow direction. Simulations were also done for an element with a sharp inlet and a large opening angle.

5. Conclusions

 A micropump designed on the basis of PZT actuator for the pumping of drug delivery has been presented. The static analysis and simulation have been performed for 2D and 3D membrane and results concludes that deflection of actuator is linear with applied potential over PZT material of the membrane. Deflection is strongly dependent on strain and stress coefficient of compliance matrices. The maximum deflection, we noticed is 6.08 μm using ANSYS and 5.58μm using intellisuite at 200 volt peak-to-peak

voltage. This deflection can be used to control the pump rate of valve less micropump for the coupled field analysis. In other hand 3D diffuser/nozzle elements have been simulated for the laminar flow to check the rate of change of flow from expansion towards the contraction and vice versa. Flow is greater at contraction and lower at expansion for the diffuser/nozzle elements.

References

[1] Microfluidic Technology and Applications,Michael Koch,Alan Evans,Arthur Brunnschweiler, Research studies press LTD,Baldock, Hertfordshire, England.

[2] FEM analysis tool ANSYS8.0.

[3] Anders Olsson, Goran Stemme, Erik Stemme, "Numerical and experimental studies of flat-walled diffuser elements for valve-less micropumps", Sensors and Actuators, Vol 84, 2000, pp. 165–175.

[4] Shifeng Li, Shaochen Chen, "Analytical analysis of a circular PZT actuator for valveless micropumps", Sensors and Actuators A, Vol. 104, 2003, pp. 151–161.

[5] Qiulian Gong), Zhaoying Zhou, Yihua Yang, Xiaohao Wang, "Design, optimization and simulation on microelectromagnetic pump", Sensors and Actuators Vol. 83, 2000, pp.200–207.

[6] Vishal Singhal, Suresh V. Garimella, Jayathi Y. Murthy, "Low Reynolds number flow through nozzle-diffuser elements in valveless micropumps", Sensors and Actuators A, Vol. 113, 2004, pp. 226–235.

[7] S.C. Chena,b, C.H. Chengc, Y.C. Lin , "Analysis and experiment of a novel actuating design with a shear mode PZT actuator for microfluidic application", Sensors and Actuators A, Vol.135, 2006, pp. 1-9.

[8] J. Darabi, C. Rhodes, "CFD modeling of an ion-drag micropump", Sensors and Actuators A, Vol. 127, 2006, pp. 94–103.

[9] Shifeng Li, Shaochen Chen, "Analytical analysis of a circular PZT actuator for valveless micropumps", Sensors and Actuators A, Vol. 104, 2003, pp.151–161.

[10] J.G. Smits, S.I. Dalke, and T.K. Cooney, "The constituent equations of piezoelectric bimorphs", Sensors and Actuators A, Vol. 28, 1991, pp. 41–61.

[11] B Fan, G. Song and F Hussain, "Simulation of a piezoelectrically actuated valveless micropump", Smart Mater. Struct. Vol. 14, 2005, pp. 400–405.

[12] Qiulian Gong), Zhaoying Zhou, Yihua Yang, Xiaohao Wang, "Design, optimization and simulation on microelectromagnetic pump", Sensors and Actuators, Vol. 83, 2000, pp. 200–207.